

This is an Open Access document downloaded from ORCA, Cardiff University's institutional repository:<https://orca.cardiff.ac.uk/id/eprint/111628/>

This is the author's version of a work that was submitted to / accepted for publication.

Citation for final published version:

Gao, Ruxin, Zhang, Yahui and Kennedy, David 2018. A hybrid boundary element-statistical energy analysis for the mid-frequency vibration of vibro-acoustic systems. *Computers and Structures* 203 , pp. 34-42. 10.1016/j.compstruc.2018.05.007

Publishers page: <http://dx.doi.org/10.1016/j.compstruc.2018.05.007>

Please note:

Changes made as a result of publishing processes such as copy-editing, formatting and page numbers may not be reflected in this version. For the definitive version of this publication, please refer to the published source. You are advised to consult the publisher's version if you wish to cite this paper.

This version is being made available in accordance with publisher policies. See <http://orca.cf.ac.uk/policies.html> for usage policies. Copyright and moral rights for publications made available in ORCA are retained by the copyright holders.



A hybrid boundary element-statistical energy analysis for the mid-frequency vibration of vibro-acoustic systems

Ruxin Gao^a, Yahui Zhang^{a*}, David Kennedy^b

^a State Key Laboratory of Structural Analysis for Industrial Equipment, Department of Engineering Mechanics, International Center for Computational Mechanics, Dalian University of Technology, Dalian 116023, PR China;

^b School of Engineering, Cardiff University, Cardiff CF24 3AA, Wales, UK

Corresponding author:

Dr. Y. H. Zhang

State Key Laboratory of Structural Analysis for Industrial Equipment, Department of Engineering Mechanics, Dalian University of Technology, Dalian 116023, PR China

Email: zhangyh@dlut.edu.cn

Tel: +86 411 84706337

Fax: +86 411 84708393

Abstract

Based on the concept of hybrid Finite Element (FE) analysis and Statistical Energy Analysis (SEA), a new hybrid method is developed for the mid-frequency vibration of vibro-acoustic systems. The Boundary Element (BE) method is used to describe the motion of a deterministic acoustic cavity. By enforcing the continuity conditions of displacement and velocity at the coupling interface, the dynamic coupling between the deterministic acoustic cavity and the statistical structure described by SEA is established. Then, a hybrid BE-SEA method for the mid-frequency vibration of vibro-acoustic systems is proposed. Post-processing provides formulations for calculating the sound pressure at points inside the acoustic cavity. Due to the nature of the BE method for acoustics, the proposed method not only has few degrees of freedom, but also automatically satisfies the Sommerfeld radiation condition at infinity for exterior acoustics problems. A numerical example compares results from the proposed hybrid BE-SEA method with those from the hybrid FE-SEA method and Monte Carlo simulation. The comparison illustrates that the proposed method gives good predictions for the mid-frequency behavior of vibro-acoustic systems and has the fewest degrees of freedom.

Keywords: Mid-frequency; Vibro-acoustics; Hybrid methodology; Boundary element method; Statistical energy analysis

1 Introduction

Vehicles such as carrier rockets, aircraft and automobiles may be subjected to a wide range of excitation frequencies during their operation. The structure and the acoustic cavities around it form a typical complex vibro-acoustic system for which it is necessary to consider the coupling interaction between the structure and the acoustic cavities. In order to improve the safety, comfort and stability of the system it is essential to study the dynamic behavior of the complex vibro-acoustic system when optimizing the design.

A complex vibro-acoustic system will typically exhibit mixed mid-frequency behavior when it is excited in a mid-frequency environment. In general, it may be difficult to study the dynamic response of complex vibro-acoustic systems by using a deterministic method such as Finite Element (FE) analysis [1, 2]. Since an appropriate element size (typically six to eight elements per wavelength [3, 4]) is required to capture the detailed deformations of the system, the degrees of freedom may increase significantly with decrease of the wavelength as the frequency increases. To overcome this difficulty, many improved methods, such as higher-order techniques [5-7], reduction techniques [8-10] and the ultra-weak variational formulation [11], have been developed based on FE analysis. However, such element-based techniques are appropriate mainly for the dynamic analysis of systems at lower frequencies. In contrast, wave based approaches can provide complete deterministic analyses. Langley [12] and Bercin and Langley [13] obtained the forced vibration responses of complex systems consisting of rectangular

plates by using the wave dynamic stiffness method. The energy flow was analyzed by Wester and Mace [14] using a wave method in which the flow of energy between components is described in terms of generalized ‘wave components’. Ma et al. [15] converted the governing differential equations for transverse vibration of thin plates into Hamiltonian canonical equations, and then proposed a semi-analytical method for steady-state forced vibration response of rectangular thin plates. Barbarulo et al. [16] developed a technique, which combines the Variational Theory of Complex Rays proposed by Ladevèze and Arnaud [17] with proper generalized decomposition, for calculating the response of acoustic systems. Desmet [18] proposed the Wave Based Method (WBM) for the steady-state dynamic analysis of vibro-acoustic systems. Higher accuracy and efficiency can be provided by these wave-based methods for predicting the system response.

However, uncertainties in the dimensions of the geometry and in the material properties inevitably arise during the manufacture and assembly of systems. As the frequency increases, the response of a system may be very sensitive to uncertainties, such as small imperfections in the system. Hence, it is necessary to consider the uncertainty of the system when it is excited in mid- and high-frequency ranges. However Monte Carlo simulation, in which both element-based and wave-based techniques can be employed to consider the uncertainty of the system, requires many reanalyses and is computationally expensive [19]. A popular statistical method is Statistical Energy Analysis (SEA) [20], in

which the system is divided into a number of subsystems according to groups of similar modes. SEA employs the time, frequency and space average energy responses of each subsystem as the degrees of freedom, and establishes the power balance equation by considering the power exchange between the subsystems. A good prediction for the statistical behavior of the system at higher frequencies may be obtained by using SEA with little time cost. However, some assumptions in SEA may only be satisfied when the system has a high modal density at higher frequencies.

Unlike SEA, the statistical modal energy distribution analysis proposed by Maxit and Guyader [21, 22] in the framework of SEA focuses on the power exchange between the modes, and not between whole subsystems. Statistical modal energy distribution analysis can be used even if the system has a low modal density, because it considers all resonant and non-resonant modes in the frequency range of interest, i.e. not just the resonant modes of the subsystem. MODal ENergy Analysis, developed by Totaro and Guyader [23] and based on the concept of the statistical modal energy distribution analysis, can provide energy analysis of subsystems at pure tone. The above two methods make a link between the energy methods and the FE method. The modal power balance equation can be established by modal analysis of the components in which the FE method models are of smaller simpler components, rather than the vibro-acoustic system as a whole. Langley [24] proposed the wave intensity method for analyzing the bending vibrations of a panel array at higher frequencies. This method provided a significant

improvement over SEA by considering the directional filtering effects of the connections, which may lead to lower statistical wavefields. Langley and Bercin [25] then extended this method to the bending and in-plane vibrations of various plate structures. For a complex system, wave intensity techniques may face some difficulty when handling complex structural joints. The energy FE method [26, 27] was developed to predict the average response of complex systems at high frequency ranges. The balance equation of the energy density is established by using net energy flow and energy superposition principles. Then, the equation can be solved using the FE method by considering the power flow between structural elements. The energy FE method can provide the local responses of the system. However the joint matrix, which was developed to deal with the discontinuity of the structures, may be difficult to obtain for complex junctions. Based on approaches describing essentially ray tracing type models [28], Le Bot [29] proposed a vibro-acoustic model for medium and high frequency analysis considering energy conservation of the systems. This model considers local variables, and can predict the repartition of energy density inside each subsystem. Tanner [30] proposed dynamical energy analysis for high frequency analysis of the vibro-acoustic systems, which interpolates between standard SEA and full ray tracing containing both these methods as limiting cases. According to this method, the typical SEA assumptions can be quantified in terms of the properties of the ray dynamics.

When a complex vibro-acoustic system is subjected to a mid-frequency excitation

force, some components are subjected to short wavelength deformation, while other components are subjected to long wavelength deformation. Considering the different vibration behaviors of components, Zhao and Vlahopoulos [31] proposed a hybrid method, which combines the FE method and the energy FE method, for analyzing co-linear beam systems. The hybrid equations of the FE subsystems and energy FE subsystems, together with the interface equations, are solved simultaneously by an iterative process. Shorter and Langley [32, 33] later presented a hybrid method combining FE and SEA for predicting the ensemble average response of complex vibro-acoustic systems. In this hybrid FE-SEA method, the FE method is employed to describe the motion of the so-called deterministic subsystems, which are subjected to long wavelength deformation, while the SEA is employed to model the so-called statistical subsystems, which are subjected to short wavelength deformation. The equations of the two types of subsystem are coupled by the diffuse-field reciprocity principle, which is a non-iterative relationship between the energy of the statistical subsystem and the cross-spectrum of the blocked reverberant force [33]. Based on the framework of hybrid FE-SEA method, Zhu et al. [34] developed the hybrid FE-energy FE method for analyzing beam-plate systems in the high frequency range. Ma et al. [35] developed a hybrid approach which employs the wave propagation method to describe the motion of rectangular plates. This method provides a good prediction for mid-frequency vibration analysis of built-up plate systems so long as the deterministic plates are rectangular. Langley and Cordioli [36] fully

discussed the application of the hybrid FE-SEA method in the mid-frequency vibration analysis of vibro-acoustic systems with domain coupling of statistical subsystems, and proposed a reduced form of the deterministic subsystem equations. However, the FE method may face some difficulty when the acoustic cavity domain is unbounded. In the hybrid method proposed by Vergote et al. [37], the WBM was adopted to model the acoustic cavity instead of the FE method, so increasing computational efficiency.

The present paper develops a hybrid approach for the mid-frequency vibration of vibro-acoustic systems within the framework of the hybrid FE-SEA method. Based on the concept of hybrid FE-SEA, the proposed method adopts the Boundary Element (BE) method [38, 39] to describe the motion of the acoustic cavity instead of the FE method or WBM. As is well known, the BE method is a powerful method for acoustics. Due to the nature of the BE method, the proposed method only discretizes the boundary of the acoustic cavity into elements, which is easier than discretizing the acoustic cavity domain and leads to a smaller number of degrees of freedom. It is also better able to handle exterior acoustics problems. Section 2 outlines the basic principles of the hybrid method. Section 3 derives the governing equation and power balance equation, followed by formulations for calculating the sound pressure at points inside the acoustic cavity. The numerical example in section 4 validates the proposed hybrid BE-SEA method against the hybrid FE-SEA and Monte Carlo simulation.

2 Basic principles of the hybrid method

In the hybrid FE-SEA method proposed by Shorter and Langley [32], a complex system is modeled as an assembly of deterministic and statistical subsystems according to deformation wavelengths. The deterministic components are modeled using the FE method, while the statistical components are modeled as SEA subsystems. The response of statistical components is viewed as the superposition of two wave fields, one of which is the direct field formed by the initial generated waves, prior to any boundary reflections, and the other is the reverberant field formed by the waves produced on the first and all subsequent reflections [33].

The presence of uncertainties in the statistical system is accounted for in the reverberant field, with the result that the direct field is deterministic across the ensemble. The direct field dynamic stiffness matrix and the blocked reverberant force can be respectively defined as those resulting from the presence of the direct field and the reverberant field. The field dynamic stiffness matrix can in principle be computed from a BE analysis. In many instances, however, analytical approaches can be used to obtain such a matrix [33]. The total dynamic stiffness matrix for the system can be found by adding the direct field dynamic stiffness of the statistical subsystems to the dynamic stiffness of the deterministic subsystems, and the total excitation applied to the system is found by adding the external excitation and the blocked reverberant force. Hence, the governing equation of the system is assembled.

The power balance equation for the reverberant field can be found by considering the conservation of energy in the statistical subsystem. The time and ensemble average input power to the direct field of the statistical subsystem can be separated into input power due to external excitation applied directly to the statistical subsystem and contributions from the force at the connection region associated with the deterministic subsystem. The power losses of the statistical subsystem are due to the rate at which work is done on the connection region by the blocked reverberant force and dissipation within the reverberant field resulting from the presence of the damping. Central to the development of the hybrid FE-SEA method is the concept of the diffuse-field reciprocity relationship [33], which relates the ensemble average of the cross-spectrum of the blocked reverberant force associated with the reverberant field to the ensemble average energy of the statistical subsystem. Then, the ensemble average rate at which energy leaves the reverberant field may be explicitly calculated as a function of the subsystem average energy as well as the ensemble average power dissipated within the reverberant field due to damping. Hence, the ensemble average energy of the subsystem can be calculated by non-iterative calculations, and once again using the diffuse-field reciprocity relationship, the ensemble average of the cross-spectrum of the response of the deterministic subsystem can be obtained.

3 Hybrid BE-SEA method for vibro-acoustic problems

Without loss of generality, this section demonstrates the hybrid BE-SEA method using a vibro-acoustic system consisting of a deterministic acoustic cavity and a statistical thin plate. The acoustic cavity is a cuboid domain with acoustically rigid walls, except for one wall, which is the vibrating plate. The displacement, pressure and normal velocity on the fluid-structure coupling interface are continuous. According to reference [33], the motion of the statistical thin plate can be partitioned into the direct field and the reverberant field, as shown in Fig. 1.

Figure 1 in text

3.1 Governing equation of the system

As described in section 2, the deterministic acoustic cavity and the direct field of the statistical thin plate are considered first to assemble the governing equation of the system.

For an acoustic cavity domain Ω , the governing differential equation for time-harmonic linear acoustics is the Helmholtz equation [38, 39]

$$\nabla^2 p(\mathbf{r}) + k_a^2 p(\mathbf{r}) = 0, \quad (1)$$

where $p(\mathbf{r})$ is the sound pressure at field point \mathbf{r} . $\nabla^2 = \frac{\partial^2}{\partial x^2} + \frac{\partial^2}{\partial y^2} + \frac{\partial^2}{\partial z^2}$ is the Laplacian operator, $k_a = \frac{\omega}{c_0}$ is the acoustic wave number, ω is the angular frequency, and c_0 is

the speed of sound.

Eq. (1) can be written in a weak formulation by applying Green's second identity [38, 39]

$$c(\mathbf{r})p(\mathbf{r}) = \int_{\Gamma} \left[p(\mathbf{r}_\Gamma) \frac{\partial G(\mathbf{r}, \mathbf{r}_\Gamma)}{\partial n(\mathbf{r}_\Gamma)} + i\rho_0\omega G(\mathbf{r}, \mathbf{r}_\Gamma)v_n(\mathbf{r}_\Gamma) \right] d\Gamma(\mathbf{r}_\Gamma), \quad (2)$$

where Γ is the boundary surface of the acoustic cavity domain Ω , $n(\mathbf{r}_\Gamma)$ and $v_n(\mathbf{r}_\Gamma)$ are the unit inward normal and the normal velocity, respectively, at the source point \mathbf{r}_Γ . ρ_0 is the density of the fluid, $i = \sqrt{-1}$ is the imaginary unit, $G(\mathbf{r}, \mathbf{r}_\Gamma)$ is the free-space Green's function for the Helmholtz equation [38, 39], $c(\mathbf{r})$ is a jump-term related to the geometry at the field point \mathbf{r} , and given by

$$c(\mathbf{r}) = \begin{cases} 1, & \mathbf{r} \in \Omega | \Gamma \\ \frac{1}{2}, & \mathbf{r} \in \Gamma(\text{smooth}) \\ \frac{\Theta}{4\pi}, & \mathbf{r} \in \Gamma(\text{nonsmooth}) \\ 0, & \mathbf{r} \notin \Omega \end{cases} \quad (3)$$

where Θ represents the solid angle which is a two-dimensional angle in the three-dimensional space that the boundary surface subtends at the field point \mathbf{r} [38, 39]. For exterior acoustics problems, similar derivation applies as for bounded domains, and the Sommerfeld radiation condition at the infinitely far boundary can be satisfied automatically. The same direct boundary integral formulation as Eq. (2) is obtained with the normal direction having a positive orientation out of the unbounded fluid domain. Eq. (2) can be discretized by dividing the boundary of the acoustic cavity into elements with

m_a nodes. For a given node $j(= 1, 2, \dots, m_a)$, the Helmholtz discrete integral equation can be written as [38, 39]

$$\begin{aligned} c(\mathbf{r}_j)p(\mathbf{r}_j) - \left(\int_{\Gamma} \mathbf{N}_a(\mathbf{r}_r) \frac{\partial G(\mathbf{r}_j, \mathbf{r}_r)}{\partial n(\mathbf{r}_r)} d\Gamma(\mathbf{r}_r) \right) \mathbf{p} \\ = i\rho_0\omega \left(\int_{\Gamma} \mathbf{N}_a(\mathbf{r}_r) G(\mathbf{r}_j, \mathbf{r}_r) d\Gamma(\mathbf{r}_r) \right) \mathbf{v}_n, \end{aligned} \quad (4)$$

where $\mathbf{N}_a(\mathbf{r}_r)$ is a row vector consisting of shape functions of boundary elements of the acoustic cavity, and vectors $\mathbf{p} \in \mathbb{C}^{m_a \times 1}$ and $\mathbf{v}_n \in \mathbb{C}^{m_a \times 1}$ respectively represent the sound pressures and the normal velocities at nodal points on the boundary of the acoustic cavity. Applying Eq. (4) at each node and ignoring the coupling interaction with the direct field of the thin plate, the BE method formulation for the acoustic cavity is obtained as the following linear system of equations

$$\mathbf{H}\mathbf{p} = \mathbf{G}\mathbf{v}_n, \quad (5)$$

where $\mathbf{H} \in \mathbb{C}^{m_a \times m_a}$ and $\mathbf{G} \in \mathbb{C}^{m_a \times m_a}$ are the influence coefficient matrices of sound pressure and normal velocity, respectively.

Consider now the governing equation of the direct field of the thin plate in the absence of the acoustic cavity. According to reference [36], the direct field of the thin plate is considered as an infinite thin plate, and a grid consisting of m_s nodes covering the coupling surface of the direct field may be required to describe the out-of-plane response of the coupling surface of the direct field of the thin plate. The uncoupled

equations of motion for the coupling surface of the direct field of the thin plate can then be written as

$$\mathbf{D}_{\text{dir}}\mathbf{u} = \mathbf{f} + \mathbf{f}_{\text{rev}}^s, \quad (6)$$

where $\mathbf{u} \in \mathbb{C}^{m_s \times 1}$ is the vector of out-of-plane displacements at nodal points on the grid of the direct field of the thin plate, $\mathbf{D}_{\text{dir}} \in \mathbb{C}^{m_s \times m_s}$ is the direct field dynamic stiffness matrix which can be given by the inverse of the receptance matrix [40, 41], $\mathbf{f} \in \mathbb{C}^{m_s \times 1}$ is the vector of generalized forces and $\mathbf{f}_{\text{rev}}^s \in \mathbb{C}^{m_s \times 1}$ is the vector of the blocked reverberant forces [32, 33].

The BE model is divided into two parts, one of which is connected to the direct field of the thin plate and is called the coupled acoustic boundary, while the other is called the uncoupled acoustic boundary. The numbers of nodes on the uncoupled acoustic boundary and coupled acoustic boundary are m_a^{nc} and m_a^{c} , respectively. Hence, the normal velocity vector can be written as $\mathbf{v}_n = (\mathbf{v}_n^{\text{ncT}}, \mathbf{v}_n^{\text{cT}})^{\text{T}}$, with $\mathbf{v}_n^{\text{nc}} \in \mathbb{C}^{m_a^{\text{nc}} \times 1}$ and $\mathbf{v}_n^{\text{c}} \in \mathbb{C}^{m_a^{\text{c}} \times 1}$ the nodal normal velocities depending on which boundary they are acting on.

Considering the coupling interaction between the acoustic cavity and the direct field of the thin plate, the direct field of the thin plate may produce an additional normal velocity $\tilde{\mathbf{v}}_n^{\text{c}} \in \mathbb{C}^{m_a^{\text{c}} \times 1}$ in the resulting BE model of Eq. (5). A relationship between the normal fluid velocity vector and the out-of-plane displacement vector of the direct field of the thin plate may be established by considering the velocity continuity at the fluid-

structure coupling interface

$$\mathbf{v}_n^c = \tilde{\mathbf{v}}_n^c = i\omega \mathbf{T}_s \mathbf{u}, \quad (7)$$

where $\mathbf{T}_s \in \mathbb{R}^{m_a^c \times m_s}$ is the transformation matrix resulting from the non-conforming grids appearing at the fluid-structure coupling face. By using Eqs. (5) and (7), the modified BE formulation for the acoustic cavity when considering the coupling interaction with the direct field of the thin plate can be written as

$$\mathbf{H}\mathbf{p} = \mathbf{G} \begin{Bmatrix} \mathbf{v}_n^{\text{nc}} \\ \tilde{\mathbf{v}}_n^c \end{Bmatrix} = \mathbf{G}(\bar{\mathbf{v}}_n + i\omega \mathbf{T}\mathbf{u}), \quad (8)$$

$$\text{with } \bar{\mathbf{v}}_n = (\mathbf{v}_n^{\text{ncT}}, \mathbf{0}_{m_s \times 1}^T)^T, \quad \mathbf{T} = \begin{bmatrix} \mathbf{0}_{m_a^{\text{nc}} \times m_s} \\ \mathbf{T}_s \end{bmatrix}.$$

The force loading of the sound pressure on the direct field of the thin plate along the fluid-structure coupling interface may be regarded as an additional normal load. By using Eq. (6), the modified out-of-plane displacement vector can be written as [37]

$$\mathbf{u} = \int_{\Gamma_s} \tilde{\mathbf{G}}(\mathbf{r}) p(\mathbf{r}) d\Gamma + \mathbf{D}_{\text{dir}}^{-1} \mathbf{f} + \mathbf{D}_{\text{dir}}^{-1} \mathbf{f}_{\text{rev}}^s, \quad (9)$$

where $\tilde{\mathbf{G}}(\mathbf{r}) = \{\tilde{G}(\mathbf{r}, \mathbf{r}_1) \quad \tilde{G}(\mathbf{r}, \mathbf{r}_2) \quad \cdots \quad \tilde{G}(\mathbf{r}, \mathbf{r}_j) \quad \cdots \quad \tilde{G}(\mathbf{r}, \mathbf{r}_{m_a^c})\}^T$ is the Green's function of the infinite thin plate and Γ_s is the coupling interface. The Green's function of the infinite thin plate is given by [40, 41]

$$\tilde{G}(\mathbf{r}, \mathbf{r}_j) = -\frac{i}{8k_b^2 D} \left[H_0^{(2)}(k_b |\mathbf{r} - \mathbf{r}_j|) - H_0^{(2)}(-ik_b |\mathbf{r} - \mathbf{r}_j|) \right], \quad (10)$$

where D is the flexural rigidity of the thin plate, k_b is the bending wave number of the thin plate and $H_0^{(2)}(\cdot)$ is the zeroth order Hankel function of the second kind. According to the BE method, $p(\mathbf{r})$ can be approximated by $p(\mathbf{r}) = \mathbf{N}_a(\mathbf{r})\mathbf{p}$, and so Eq. (9) can be written as

$$\mathbf{u} = \left(\int_{\Gamma_S} \tilde{\mathbf{G}}(\mathbf{r})\mathbf{N}_a(\mathbf{r})d\Gamma \right) \mathbf{p} + \mathbf{D}_{\text{dir}}^{-1}\mathbf{f} + \mathbf{D}_{\text{dir}}^{-1}\mathbf{f}_{\text{rev}}^S. \quad (11)$$

Pre-multiplying Eq. (11) by \mathbf{D}_{dir} gives

$$\mathbf{D}_{\text{dir}}\mathbf{u} = \mathbf{f} + \mathbf{f}_{\text{rev}}^S + \mathbf{A}\mathbf{p}, \quad (12)$$

with

$$\mathbf{A} = \mathbf{D}_{\text{dir}} \int_{\Gamma_S} \tilde{\mathbf{G}}(\mathbf{r})\mathbf{N}_a(\mathbf{r})d\Gamma. \quad (13)$$

The governing equation of the system can be obtained by combining Eqs. (8) and (12), and is written as

$$\begin{bmatrix} \mathbf{H} & -i\omega\mathbf{G}\mathbf{T} \\ -\mathbf{A} & \mathbf{D}_{\text{dir}} \end{bmatrix} \begin{Bmatrix} \mathbf{p} \\ \mathbf{u} \end{Bmatrix} = \begin{Bmatrix} \mathbf{G}\bar{\mathbf{v}}_n \\ \mathbf{f} \end{Bmatrix} + \begin{Bmatrix} \mathbf{0}_{m_a \times 1} \\ \mathbf{f}_{\text{rev}}^S \end{Bmatrix}. \quad (14)$$

For the sake of simplicity, Eq. (14) will be written as

$$\mathbf{D}_{\text{tot}}\mathbf{q} = \mathbf{f}_{\text{ext}} + \mathbf{f}_{\text{rev}}, \quad (15)$$

where $\mathbf{D}_{\text{tot}} = \begin{bmatrix} \mathbf{H} & -i\omega\mathbf{G}\mathbf{T} \\ -\mathbf{A} & \mathbf{D}_{\text{dir}} \end{bmatrix}$ is the total dynamic stiffness matrix, $\mathbf{q} = \begin{Bmatrix} \mathbf{p} \\ \mathbf{u} \end{Bmatrix}$ is the

vector of all degrees of freedom, $\mathbf{f}_{\text{ext}} = \begin{Bmatrix} \mathbf{G}\bar{\mathbf{v}}_n \\ \mathbf{f} \end{Bmatrix}$ is the vector of all external forces and $\mathbf{f}_{\text{rev}} = \begin{Bmatrix} \mathbf{0}_{m_a \times 1} \\ \mathbf{f}_{\text{rev}}^s \end{Bmatrix}$ is the vector of all blocked reverberant forces.

3.2 Power balance equation

According to reference [33], if there is sufficient uncertainty in the statistical thin plate, the statistics of the blocked reverberant force tend to zero. Rewriting Eq. (15) in cross-spectral form and averaging over an ensemble of statistical thin plate gives [32, 33]

$$\mathbf{S}_{qq} = \langle \mathbf{q}\mathbf{q}^H \rangle = \mathbf{S}_{qq}^{\text{ext}} + \mathbf{S}_{qq}^{\text{rev}}, \quad (16)$$

where $\langle \cdot \rangle$ is the ensemble average, \cdot^H is the Hermitian transpose of \cdot , and

$$\mathbf{S}_{qq}^{\text{ext}} = \mathbf{D}_{\text{tot}}^{-1} \mathbf{S}_{ff}^{\text{ext}} \mathbf{D}_{\text{tot}}^{-H} = \begin{bmatrix} \mathbf{S}_{pp}^{\text{ext}} & \mathbf{S}_{pu}^{\text{ext}} \\ \mathbf{S}_{up}^{\text{ext}} & \mathbf{S}_{uu}^{\text{ext}} \end{bmatrix}, \quad (17)$$

$$\mathbf{S}_{qq}^{\text{rev}} = \mathbf{D}_{\text{tot}}^{-1} \mathbf{S}_{ff}^{\text{rev}} \mathbf{D}_{\text{tot}}^{-H} = \begin{bmatrix} \mathbf{S}_{pp}^{\text{rev}} & \mathbf{S}_{pu}^{\text{rev}} \\ \mathbf{S}_{up}^{\text{rev}} & \mathbf{S}_{uu}^{\text{rev}} \end{bmatrix}, \quad (18)$$

where the subscripts p and u stand for the degrees of freedom of acoustic cavity and the direct field of the thin plate, respectively. \cdot^{-H} is the Hermitian transpose of the inverse matrix. $\mathbf{S}_{ff}^{\text{ext}}$ and $\mathbf{S}_{ff}^{\text{rev}}$ are the cross-spectrum matrices of the vector of total external forces and total blocked reverberant forces, respectively. By using Eqs. (14) and (15), $\mathbf{S}_{ff}^{\text{ext}}$ and $\mathbf{S}_{ff}^{\text{rev}}$ can be, respectively, written as

$$\mathbf{S}_{ff}^{\text{ext}} = \langle \mathbf{f}_{\text{ext}} \mathbf{f}_{\text{ext}}^H \rangle, \quad (19)$$

$$\mathbf{S}_{ff}^{\text{rev}} = \langle \mathbf{f}_{\text{rev}} \mathbf{f}_{\text{rev}}^{\text{H}} \rangle = \begin{bmatrix} \mathbf{0}_{m_a \times m_a} & \mathbf{0}_{m_a \times m_s} \\ \mathbf{0}_{m_s \times m_a} & \mathbf{S}_{ff}^{\text{rev},s} \end{bmatrix}, \quad (20)$$

with $\mathbf{S}_{ff}^{\text{rev},s} = \langle \mathbf{f}_{\text{rev}}^s \mathbf{f}_{\text{rev}}^{s\text{H}} \rangle$. A connection between the ensemble average of the cross-spectrum $\mathbf{S}_{ff}^{\text{rev},s}$ of blocked reverberant force and the ensemble average of the energy E of the direct field of the thin plate may be established by the diffuse field reciprocity principle [33]. It can be written as

$$\mathbf{S}_{ff}^{\text{rev},s} = \frac{4E}{\pi\omega n_m} \text{Im}\{\mathbf{D}_{\text{dir}}\}, \quad (21)$$

where n_m is the modal density of the thin plate. Combining Eqs. (18), (20) and (21) gives

$$\mathbf{S}_{qq}^{\text{rev}} = \frac{E}{n_m} \mathbf{K}, \quad (22)$$

where

$$\mathbf{K} = \frac{4}{\pi\omega} \mathbf{D}_{\text{tot}}^{-1} \text{Im}\{\tilde{\mathbf{D}}_{\text{dir}}\} \mathbf{D}_{\text{tot}}^{-\text{H}}, \quad (23)$$

with

$$\tilde{\mathbf{D}}_{\text{dir}} = \begin{bmatrix} \mathbf{0}_{m_a \times m_a} & \mathbf{0}_{m_a \times m_s} \\ \mathbf{0}_{m_s \times m_a} & \mathbf{D}_{\text{dir}} \end{bmatrix}. \quad (24)$$

Matrix \mathbf{K} can be written in block form as

$$\mathbf{K} = \begin{bmatrix} \mathbf{K}_{pp} & \mathbf{K}_{pu} \\ \mathbf{K}_{up} & \mathbf{K}_{uu} \end{bmatrix}. \quad (25)$$

The power balance equation of the reverberant field of the thin plate can be written as

$$P_{\text{in}} = P_{\text{out}}^{\text{rev}} + P_{\text{diss}}, \quad (26)$$

where $P_{\text{in}} = P_{\text{in}}^{\text{dir}} + P_{\text{in}}^{\text{ext}}$ is the total power input to the statistical thin plate, with $P_{\text{in}}^{\text{dir}}$ the power arising from the force applied to the deterministic acoustic cavity, and $P_{\text{out}}^{\text{rev}}$ the power caused by other sources (such as rain-on-the-roof excitation) applied directly to the statistical thin plate. P_{diss} is the power dissipated in the statistical thin plate, for which proportional damping is assumed in the SEA.

The time and ensemble average input power to the direct field is given by

$$P_{\text{in}}^{\text{dir}} = \frac{\omega}{2} \sum_{ij} \text{Im}\{\mathbf{D}_{\text{dir},ij}\} (\mathbf{S}_{uu}^{\text{ext}})_{ij}. \quad (27)$$

The ensemble average power dissipated within the reverberant field of the thin plate can be written as [20]

$$P_{\text{diss}} = \omega\eta E, \quad (28)$$

where η is the damping loss factor of the thin plate.

The rate at which work is done on the connection region by the blocked reverberant force determines the ensemble average rate at which energy leaves the reverberant field

of the thin plate [37]

$$P_{\text{out}}^{\text{rev}} = \frac{1}{2} \text{Re} \left\{ \int_{\Gamma_S} p_{\text{rev}}(\mathbf{r}) v_{n,\text{rev}}^*(\mathbf{r}) d\Gamma \right\}, \quad (29)$$

where $p_{\text{rev}}(\mathbf{r})$ and $v_{n,\text{rev}}(\mathbf{r})$ are the sound pressure and normal velocity, respectively, at the coupling interface due to the blocked reverberant force. $*$ stands for the conjugate of \cdot . Considering the velocity continuity at the coupling interface, Eq. (29) can be written as

$$P_{\text{out}}^{\text{rev}} = \frac{1}{2} \text{Re} \left\{ -i\omega \int_{\Gamma_S} [\mathbf{N}_s(\mathbf{r}) \mathbf{u}_{\text{rev}}]^\text{H} [\mathbf{N}_a(\mathbf{r}) \mathbf{p}_{\text{rev}}] d\Gamma \right\}, \quad (30)$$

where \mathbf{p}_{rev} and \mathbf{u}_{rev} are the vectors of sound pressure on the boundary of the acoustic cavity and out-of-plane displacement of the direct field of the thin plate, respectively, due to the blocked reverberant force, $\mathbf{N}_s(\mathbf{r}_\Gamma)$ is a row vector consisting of shape functions for the out-of-plane displacement of the direct field of the thin plate. Simplifying Eq. (30) gives

$$P_{\text{out}}^{\text{rev}} = \frac{1}{2} \text{Re} \left\{ -i\omega \sum_{ij} \left(\int_{\Gamma_S} \mathbf{N}_s^\text{H}(\mathbf{r}) \mathbf{N}_a(\mathbf{r}) d\Gamma \right)_{ij} (\mathbf{S}_{up}^{\text{rev}})_{ij}^* \right\}. \quad (31)$$

By using Eqs. (18), (22)-(25) and (31), the time and ensemble average power leaving the reverberant field of the thin plate are given by

$$P_{\text{out}}^{\text{rev}} = h_{\text{out}}^{\text{rev}} \frac{E}{n_m}, \quad (32)$$

with

$$h_{\text{out}}^{\text{rev}} = \frac{1}{2} \text{Re} \left\{ -i \sum_{ij} \left(\int_{\Gamma_s} \mathbf{N}_s^{\text{H}}(\mathbf{r}) \mathbf{N}_a(\mathbf{r}) d\Gamma \right)_{ij} (\mathbf{K}_{up})_{ij}^* \right\}. \quad (33)$$

Inserting Eqs. (27), (28) and (32) into Eq. (26) gives the following expression for power balance within the reverberant field of the thin plate

$$C \frac{E}{n_m} = P, \quad (34)$$

with $C = \omega n_m \eta + h_{\text{out}}^{\text{rev}}$, $P = P_{\text{in}}^{\text{dir}} + P_{\text{in}}^{\text{ext}}$.

3.3 Post-processing

The energy of the thin plate can be calculated using the power balance equation, i.e. Eq. (34), and then the response cross-spectrum of the system may be obtained by using Eqs. (16)-(24). In the above derivation, however, the results associated with the acoustic cavity only give the responses on its boundary. By using Eq. (4), formulations for calculating the response of sound pressure for any point inside the acoustic cavity domain can be obtained, as follows.

Selecting some points inside the acoustic cavity domain, the matrices \mathbf{g} and \mathbf{h} containing the coefficient vectors of the sound pressure and normal velocity, respectively,

can be obtained by using Eq. (4). Then the vector of the sound pressures at the selected points inside the acoustic cavity can be written as

$$\mathbf{p}_{\text{int}} = \mathbf{g}(\bar{\mathbf{v}}_n + i\omega\mathbf{T}\mathbf{u}) - \mathbf{h}\mathbf{p}. \quad (35)$$

Rewriting Eq. (35) in cross-spectral form and averaging over an ensemble of the statistical thin plate gives

$$\begin{aligned} \mathbf{S}_{pp}^{\text{int}} = & \omega^2(\mathbf{g}\mathbf{T}\mathbf{S}_{uu}\mathbf{T}^H\mathbf{g}^H) + \mathbf{g}\mathbf{S}_{\bar{\mathbf{v}}_n\bar{\mathbf{v}}_n}\mathbf{g}^H + \mathbf{h}\mathbf{S}_{pp}\mathbf{h}^H \\ & + i\omega(\mathbf{\Delta} - \mathbf{\Delta}^H + \mathbf{\Xi} - \mathbf{\Xi}^H) - \mathbf{\Pi} - \mathbf{\Pi}^H, \end{aligned} \quad (36)$$

where

$$\mathbf{\Delta} = \mathbf{g}\mathbf{T}\mathbf{S}_{u\bar{\mathbf{v}}_n}\mathbf{g}^H, \quad (37)$$

$$\mathbf{\Xi} = \mathbf{h}\mathbf{S}_{pu}\mathbf{T}^H\mathbf{g}^H, \quad (38)$$

$$\mathbf{\Pi} = \mathbf{g}\mathbf{S}_{\bar{\mathbf{v}}_np}\mathbf{h}^H, \quad (39)$$

with $\mathbf{S}_{uu} = \langle \mathbf{u}\mathbf{u}^H \rangle$, $\mathbf{S}_{\bar{\mathbf{v}}_n\bar{\mathbf{v}}_n} = \langle \bar{\mathbf{v}}_n\bar{\mathbf{v}}_n^H \rangle$, $\mathbf{S}_{pp} = \langle \mathbf{p}\mathbf{p}^H \rangle$, $\mathbf{S}_{u\bar{\mathbf{v}}_n} = \langle \mathbf{u}\bar{\mathbf{v}}_n^H \rangle$, $\mathbf{S}_{pu} = \langle \mathbf{p}\mathbf{u}^H \rangle$ and $\mathbf{S}_{\bar{\mathbf{v}}_np} = \langle \bar{\mathbf{v}}_n\mathbf{p}^H \rangle$. $\mathbf{S}_{\bar{\mathbf{v}}_n\bar{\mathbf{v}}_n}$ can be conveniently obtained from the specified normal velocity on the boundary of the acoustic cavity. \mathbf{S}_{pp} , \mathbf{S}_{uu} and \mathbf{S}_{pu} can be calculated using the formulations given in the previous section. In what follows, the formulations for calculating $\mathbf{S}_{u\bar{\mathbf{v}}_n}$ and $\mathbf{S}_{\bar{\mathbf{v}}_np}$ are obtained using Eq. (8).

Post-multiplying Eq. (8) by \mathbf{p}^H gives

$$\mathbf{Hpp}^H = \mathbf{G}(\bar{\mathbf{v}}_n + i\omega\mathbf{T}\mathbf{u})\mathbf{p}^H. \quad (40)$$

Simplifying Eq. (40) and averaging over an ensemble of the statistical thin plate gives

$$\mathbf{S}_{\bar{v}_n p} = \mathbf{G}^{-1}\mathbf{HS}_{pp} - i\omega\mathbf{TS}_{pu}^H. \quad (41)$$

Similarly, post-multiplying Eq. (8) by $\bar{\mathbf{v}}_n^H$, and averaging over an ensemble of the statistical thin plate gives

$$\mathbf{S}_{u\bar{v}_n} = \mathbf{T}^{-1}(\mathbf{G}^{-1}\mathbf{HS}_{p\bar{v}_n} - \mathbf{S}_{\bar{v}_n\bar{v}_n}^H)/i\omega. \quad (42)$$

It is important to note here that the transformation matrix \mathbf{T} is generally not invertible.

But Eq. (42) can be used as

$$\mathbf{TS}_{u\bar{v}_n} = (\mathbf{G}^{-1}\mathbf{HS}_{p\bar{v}_n} - \mathbf{S}_{\bar{v}_n\bar{v}_n}^H)/i\omega. \quad (43)$$

Inserting Eqs. (41) and (43) into Eq. (36), the cross-spectrum of the sound pressure at the points inside the acoustic cavity can be obtained, and then the ensemble average of sound pressure amplitude may be calculated.

4 Numerical example

In this section, a simple verification example consisting of an acoustic cavity and a

thin plate, as shown in Fig. 2, is presented for illustrating the validity of proposed method. The acoustic cavity filled with air has dimensions 0.7 m by 1.0 m by 0.5 m. At one side a thin aluminum plate with dimensions of 0.7 m by 1.0 m by 0.001m is connected, and the other walls are considered to be acoustically rigid. The edges of the plate are all simply supported. The mass density and sound speed of the air are $\rho_0 = 1.225 \text{ kg/m}^3$ and $c_0 = 340.0 \text{ m/s}$, respectively. The mass density, Young's modulus, Poisson's ratio and damping loss factor of the plate are $\rho_p = 2700.0 \text{ kg/m}^3$, $E = 71.0 \text{ GPa}$, $\nu = 0.33$ and $\eta = 0.01$, respectively. A unit velocity is applied over a surface of 0.04 m^2 on the front wall of the acoustic cavity located at the point (0.2, 0.3, 0.5), and the frequency range considered is from 1 Hz to 400 Hz.

Figure 2 in text

In the frequency range of interest, the acoustic cavity only has 7 modes, while the thin plate has 79 modes. Since there are significant differences between the modal density of the acoustic cavity and the thin plate, the system will possess typical mid-frequency vibration behavior, here with a deterministic acoustical behavior and a statistical structural behavior, within the frequency range. The results obtained using the proposed hybrid BE-SEA method are benchmarked by comparison to models of the hybrid FE-SEA method [33] and large FE Monte Carlo simulation.

The acoustic cavity is modeled by using the BE method and FE method, respectively, in the hybrid BE-SEA and hybrid FE-SEA models, while the thin plate is modeled by SEA in both methods. In order to obtain acceptable results, a very fine FE mesh is used to capture short wavelengths in the Monte Carlo simulation model of the system. An ensemble is generated by adding 20% of the mass of the thin plate at 200 points, which are chosen randomly, within the thin plate. The acoustic system matrices and the acoustic-structure system matrices in respectively the hybrid FE-SEA method and the Monte Carlo simulation are composed using NX Nastran 10.0 [42]. It is important to note that appropriate element sizes were chosen for the parts modeled using element-based techniques in the three methods, typically six to eight elements per wavelength. The acoustic cavity model employed in the hybrid BE-SEA method has fewer degrees of freedom than those employed both in the hybrid FE-SEA method and in the Monte Carlo simulation, as shown in Fig. 3. Details of the parts modeled using element-based techniques in the three methods are given in Table 1.

Figure 3 in text

Table 1 in text

In order to verify the proposed method, 500 sets of random point masses have been

added to the FE model of the thin plate employed in the Monte Carlo simulation, and the results from each of these systems are shown in Fig. 4, together with the average of the 500 results. The results calculated with the proposed method and hybrid FE-SEA method are also shown in Fig. 4. As can be seen, the results obtained from the proposed method have a good agreement with the results from the hybrid FE-SEA method and predict the same variation tendency as the results from the Monte Carlo simulation. However, it can be seen from Fig. 4 that there are small discrepancies at lower frequencies due to the weak randomness in the thin plate. As the frequency increases, both hybrid approaches predict well the averaged results of the Monte Carlo simulation with perturbed mass of the thin plate.

Figure 4 in text

The BE method is employed for modeling the acoustic cavity in the proposed method. Modeling the boundary of an acoustic cavity using the BE method is always easier than modeling the acoustic cavity itself using the FE method, not to mention that the acoustic cavity may be unbounded in an exterior acoustics problem. The reduction of dimensions due to using the BE method implies the proposed method will be more efficient than the hybrid FE-SEA method in the modeling stage. Compared with the hybrid WBM-SEA method [37], the proposed method can handle a more complex boundary of the geometry,

and has better numerical stability. Of course, since the Green's function employed in the hybrid BE-SEA method is frequency dependent, the coefficient matrices in the boundary element equation are also frequency dependent. This results in a very time consuming frequency dependent analysis because the coefficient matrices have to be calculated at each frequency. Moreover, although the BE method allows for a more compact problem description and easier mesh generation, it generates fully populated and unsymmetric matrices, which means that the computation time is longer compared to the sparse, symmetric matrices which arise in the FE method.

In order to further verify the proposed method, Fig. 5 compares the sound pressure contours on the boundary of the acoustic cavity obtained by using the proposed method and Monte Carlo simulation at 235Hz. A good agreement between two contours can be seen, except for some localized small discrepancies due to the different element sizes. Fig. 6 shows the sound pressure at the center of the surface subjected to external excitation calculated by the present method and Monte Carlo simulation. As can be seen, the proposed approach yields a good prediction of the response of the sound pressure amplitude, with statistical smoothing of the effect of the each realization in the ensemble.

Figure 5 in text

Figure 6 in text

In order to verify the formulations of the post-processing, comparison of the sound pressure amplitudes at the point (0.40, 0.60, 0.30) inside the acoustic cavity obtained by using the proposed method and the Monte Carlo method are shown in Fig. 7. Good agreements can be found in the comparison. However, it can be seen from Fig. 7 that there are apparent discrepancies at lower frequencies because of the weakness of the randomness. As the frequency increases, the proposed method predicts well the averaged results of the Monte Carlo simulation with perturbed mass of the thin plate.

Figure 7 in text

As can be seen in Figs. 6 and 7, the 500 sound pressure-frequency curves obtained from the Monte Carlo simulation are relatively concentrated. This is because the acoustic wavelength of the cavity is still long while the deformation wavelength of the thin plate become very short at 400Hz. As explained earlier, the uncertainty can be ignored when the system has a large wavelength at a lower frequency range. However, it should be considered when the system has small wavelength at mid- and high-frequency ranges. Moreover, the response curves computed using a fully deterministic FE model, for a completely rigid plate and for a homogenous thin plate with nominal thickness, are shown in Figs. 6 and 7. As can be seen in Figs. 6 and 7, although the sound pressure level

considering the plate as a rigid plate is similar to that considering the plate as a flexible thin plate, the frequencies at which the peaks of the sound pressure appear in the two circumstances are obviously different. The response curve computed considering the plate as a flexible thin plate has more peaks than that considering the plate as a rigid plate, which is caused by the dense modes of the plate in the frequency band of interest. The hybrid BE-SEA method assumes that the statistical subsystem has sufficient uncertainty [32, 33]. The plate with fully deterministic parameters may be considered as a special case of a collection of fully random plates. Hence, in theory, the response curve computed considering the plate as a homogenous thin plate should be enveloped in the curve set computed using Monte Carlo simulation with enough realizations. However, it is important to note that the uncertainty in the Monte Carlo simulation in the numerical example is applied by adding 20% of the mass of the thin plate at 200 points, which are chosen randomly, within the thin plate. This will result a slight decrease in the natural frequencies of the system, which can be seen in Figs. 6 and 7.

5 Conclusions

A hybrid method based on the concept of the hybrid FE-SEA has been proposed for the mid-frequency vibration of vibro-acoustic systems. In the proposed method the deterministic acoustic cavity is modeled by using the BE method. Due to the nature of the BE method, the proposed method is more efficient in the modeling stage, and

automatically satisfies the Sommerfeld radiation condition at the infinitely far boundary for exterior acoustics problems. It should be pointed out that the coefficient matrices in the boundary element equation are frequency dependent, which results in a very time consuming frequency dependent analysis because these coefficient matrices have to be calculated at each frequency. Moreover, unlike the hybrid FE-SEA method, the present method generates a linear system of equations with a dense unsymmetric matrix. Hence, much time may be required to solve that equation. A typical vibro-acoustic system consisting of an acoustic cavity and a thin plate is considered as a numerical example. For the ensemble average of the energy stored by the thin plate and sound pressure at the boundary and inside the acoustic cavity, the results of the proposed method agree well with those obtained by the hybrid FE-SEA method and Monte Carlo simulation. Furthermore, the degree of energy dispersion of the thin plate and sound pressure of the acoustic cavity computed using Monte Carlo approach for 500 realizations of ensemble shows that the random uncertainty of thin plate has great influence on itself, but very little influence on the acoustic cavity. Hence, it is necessary to take into account random uncertainty in modeling short-wavelength motion.

Acknowledgments

The authors are grateful for support under grants from the National Science Foundation of China (11672060) and the Cardiff University Advanced Chinese

Engineering Centre.

References

- [1] Zienkiewicz OC, Taylor RL. The Finite Element Method. 5th ed. Boston: Butterworth-Heinemann; 2000.
- [2] Bathe KJ. Finite Element Procedures. Upper Saddle River: Prentice Hall; 1996.
- [3] Steel JA, Craik RJM. Statistical energy analysis of structure-borne sound transmission by finite element methods. *Journal of Sound and Vibration* 1994; 178(4): 553-561.
- [4] Simmons C. Structure-borne sound transmission through plate junctions and estimates of sea coupling loss factor using the finite element method. *Journal of Sound and Vibration* 1991; 144(2): 215-227.
- [5] Koshiba M, Maruyama S, Hirayama K. A vector finite element method with the high-order mixed-interpolation-type triangular elements for optical waveguiding problems. *Journal of Lightwave Technology* 1994; 12(3): 495-502.
- [6] Harari I, Avraham D. High-order finite element methods for acoustic problems. *Journal of Computational Acoustics* 1997; 5(1): 33-51.
- [7] Dey S, Shirron JJ, Couchman LS. Mid-frequency structural acoustic and vibration analysis in arbitrary, curved three-dimensional domains. *Computers and Structures* 2001; 79(6): 617-629.

- [8] Craig RR Jr. Substructure method in vibration. *Journal of Vibration and Acoustics* 1995; 117: 207-213.
- [9] Donders S, Pluymers B, Ragnarsson P, Hadjit R, Desmet W. The wave-based substructuring approach for the efficient description of interface dynamics in substructuring. *Journal of Sound and Vibration* 2010; 329(8): 1062-1080.
- [10] Ko JH, Byun D. Comparison on numerical solutions for mid-frequency response analysis of finite element linear systems. *Computers and Structures* 2010; 88(1-2): 18-24.
- [11] Cessenat O, Després B. Using plane waves as base functions for solving time harmonic equations with the ultra weak variational formulation. *Journal of Computational Acoustics* 2003; 11(2): 227-238.
- [12] Langley RS. Application of the dynamic stiffness method to the free and forced vibrations of aircraft panels. *Journal of Sound and Vibration* 1989; 135(2): 319-331.
- [13] Bercin AN, Langley RS. Application of the dynamic stiffness technique to the in-plane vibrations of plate structures. *Computers and Structures* 1996; 59(5): 869-875.
- [14] Wester ECN, Mace BR. Wave component analysis of energy flow in complex structures - Part I: A deterministic model. *Journal of Sound and Vibration* 2005; 285(1-2): 209-227.
- [15] Ma Y, Zhang Y, Kennedy D. A symplectic analytical wave based method for the wave propagation and steady state forced vibration of rectangular thin plates. *Journal of*

Sound and Vibration 2015; 339: 196-214.

[16] Barbarulo A, Ladevèze P, Riou H, Kovalevsky L. Proper Generalized Decomposition applied to linear acoustic: A new tool for broad band calculation. Journal of Sound and Vibration 2014; 333(11): 2422-2431.

[17] Ladevèze P, Arnaud L. New computational method for structural vibrations in the medium-frequency range. Computer Assisted Mechanics and Engineering Sciences 2000; 7(2): 219-226.

[18] Desmet W. A wave based prediction technique for coupled vibro-acoustic analysis, K.U.Leuven, division PMA, PhD. Thesis 98D12. http://www.mech.kuleuven.be/mod/wbm/phd_dissertations/.

[19] Cotoni V, Shorter PJ, Langley RS. Numerical and experimental validation of a finite element-statistical energy analysis method. Journal of the Acoustical Society of America 2007; 122: 259-270.

[20] Lyon RH, DeJong RG. Theory and Application of Statistical Energy Analysis. 2nd ed. Boston: Butterworth-Heinemann; 1995.

[21] Maxit L, Guyader JL. Estimation of sea coupling loss factors using a dual formation and FEM modal information, Part I: theory. Journal of Sound and Vibration 2001; 239(5): 907-930.

[22] Maxit L, Guyader JL. Estimation of sea coupling loss factors using a dual formation and FEM modal information, Part II: numerical applications. Journal of Sound and

- Vibration 2001; 239(5): 931-948.
- [23] Totaro N, Guyader JL. MODal ENergy analysis. Journal of Sound and Vibration 2013; 332(16): 3735-3749.
- [24] Langley RS. A wave intensity technique for the analysis of high frequency vibrations. Journal of Sound and Vibration 1992; 159(3): 483-502.
- [25] Langley RS, Bercin AN. Wave intensity analysis of high frequency vibrations. Philosophical Transactions of the Royal Society London A 1994; 346: 489-499.
- [26] Nefske DJ, Sung SH. Power flow finite element analysis of dynamic systems: basic theory and application to beams. Journal of Vibration and Acoustics 1989; 111(1): 94-100.
- [27] Wang S, Bernhard RJ. Theory and applications of a simplified energy finite element method and its similarity to SEA. Noise Control Engineering Journal 2002; 50(2): 63-72.
- [28] Glasser AS (Ed.). An Introduction to Ray Tracing. New York: Academic Press; 1989.
- [29] Le Bot A. A vibroacoustic model for high frequency analysis. Journal of Sound and Vibration 1998; 211(4): 537-554.
- [30] Tanner G. Dynamical energy analysis - determining wave energy distributions in vibro-acoustical structures in the high-frequency regime. Journal of Sound and Vibration 2009; 320(4-5): 1023-1038.
- [31] Zhao X, Vlahopoulos N. A hybrid finite element formulation for mid-frequency

- analysis of systems with excitation applied on short members. *Journal of Sound and Vibration* 2000; 237(2): 181-202.
- [32] Shorter PJ, Langley RS. Vibro-acoustic analysis of complex systems. *Journal of Sound and Vibration* 2005; 288(3): 669-699.
- [33] Shorter PJ, Langley RS. On the reciprocity relationship between direct field radiation and diffuse reverberant loading. *Journal of the Acoustical Society of America* 2005; 117(1): 85-95.
- [34] Zhu D, Chen H, Kong X, Zhang W. A hybrid finite element-energy finite element method for mid-frequency vibrations of built-up structures under multi-distributed loadings. *Journal of Sound and Vibration* 2014; 333(22): 5723-5745.
- [35] Ma Y, Zhang Y, Kennedy D. A hybrid wave propagation and statistical energy analysis on the mid-frequency vibration of built-up plate systems. *Journal of Sound and Vibration* 2015; 352: 63-79.
- [36] Langley RS, Cordioli JA. Hybrid deterministic-statistical analysis of vibro-acoustic systems with domain couplings on statistical components. *Journal of Sound and Vibration* 2009; 321(3-5): 893-912.
- [37] Vergote K, Van Genechten B, Vandepitte D, Desmet W. On the analysis of vibro-acoustic systems in the mid-frequency range using a hybrid deterministic-statistical approach. *Computers and Structures* 2011; 89(11-12): 868-877.
- [38] Wu TW. *Boundary Element Acoustics: Fundamentals and Computer Codes*.

Southampton: WIT; 2000.

[39] Ciskowski RD, Brebbia CA. Boundary Element Methods in Acoustics. Southampton:

Computational Mechanics Publications; 1991.

[40] Cremer L, Heckl M, Petersson BAT. Structure-borne Sound. 3rd ed. Berlin: Springer;

2005.

[41] Filippi PJT. Vibrations and Acoustic Radiation of Thin Structures: Physical Basis,

Theoretical Analysis and Numerical Methods. Hoboken: John Wiley & Sons, Inc;

2008.

[42] Siemens Product Lifecycle Management Software Inc. NX Nastran User's Guide.

Munich: Siemens AG; 2014.

Table captions

Table 1 Details of the parts modeled using element-based techniques

Tables

Table 1 Details of the parts modeled using element-based techniques

Analysis model		Element type	Element size (m)	Number of elements per wavelength at 400Hz	Number of degrees of freedom
Hybrid BE-SEA	Cavity	4-node quadrilateral	0.050	17	1242
	Direct field	4-node quadrilateral	0.025	6	1189
Hybrid FE-SEA	Cavity	8-node hexahedral	0.050	17	3465
	Direct field	4-node quadrilateral	0.025	6	1189
Monte Carlo simulation	Cavity	8-node hexahedral	0.020	42	47736
	Plate	4-node quadrilateral	0.020	6	5508

Figure captions

Fig. 1 Model of a vibro-acoustic system. Left, acoustic cavity; middle, direct field; right, reverberant field.

Fig. 2 Problem geometry. Gray area, a thin plate coupled to the acoustic cavity; blue area, the domain subjected to external excitation; other areas, the acoustically rigid walls.

Fig. 3 The models of the acoustic cavity employed in the three methods

Fig. 4 Energy in the plate. Gray lines, computed using Monte Carlo approach for 500 realizations of ensemble; black line, ensemble average of Monte Carlo results; red line, ensemble average computed using Hybrid FE-SEA method; blue line, ensemble average computed using Hybrid BE-SEA method.

Fig. 5 Sound pressure contour on the boundary of acoustic cavity.

Fig. 6 Sound pressure response at the center of the domain subjected to external excitation. Gray lines, computed using Monte Carlo approach for 500 realizations of ensemble; red line, ensemble average of Monte Carlo results; blue line, ensemble average computed using Hybrid BE-SEA method; black line, computed using a fully deterministic FE model considering the plate as a rigid plate; dark cyan line, computed using a fully deterministic FE model considering the plate as a homogenous plate with the nominal thickness provided by this paper.

Fig. 7 Sound pressure response at a point inside the acoustic cavity with coordinates (0.40, 0.60, 0.30). Gray lines, computed using Monte Carlo approach for 500 realizations

of ensemble; red line, ensemble average of Monte Carlo results; blue line, ensemble average computed using Hybrid BE-SEA method; black line, computed using a fully deterministic FE model considering the plate as a rigid plate; dark cyan line, computed using a fully deterministic FE model considering the plate as a homogenous plate with the nominal thickness provided by this paper.

Figures

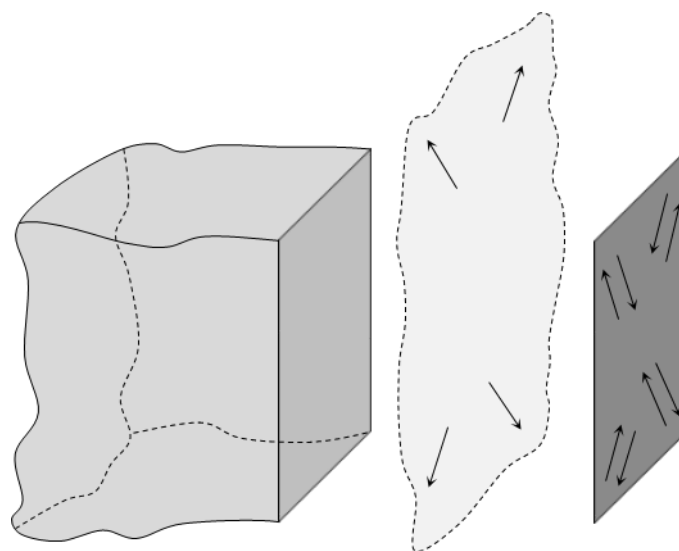


Fig. 1 Model of a vibro-acoustic system. Left, acoustic cavity; middle, direct field;
right, reverberant field.

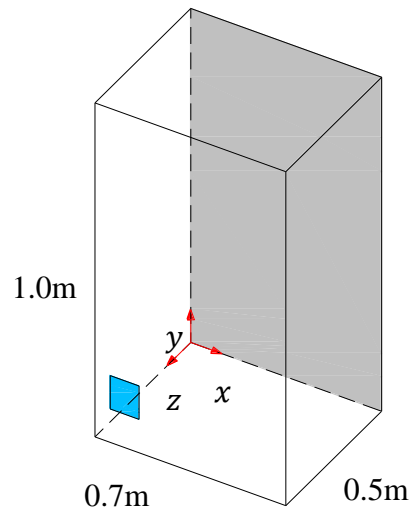
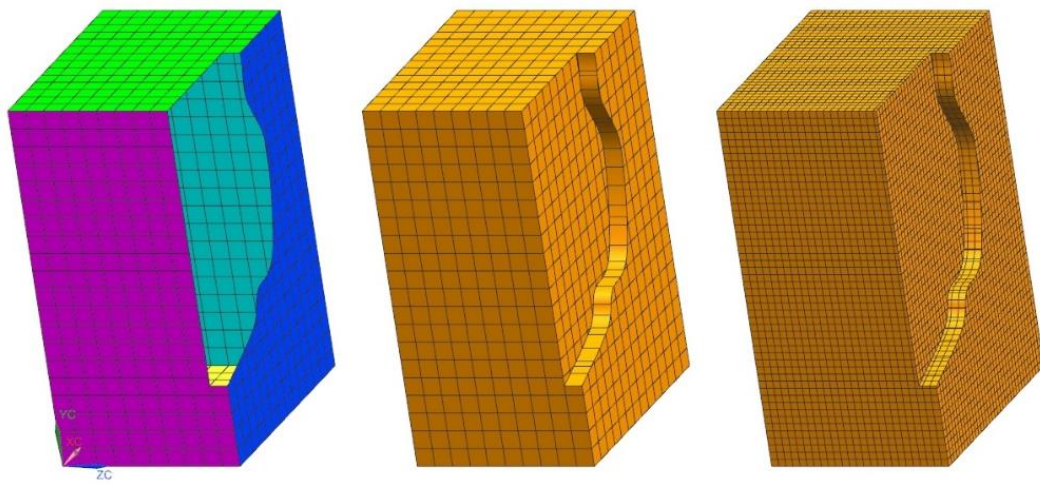


Fig. 2 Problem geometry. Gray area, a thin plate coupled to the acoustic cavity; blue area, the domain subjected to external excitation; other areas, the acoustically rigid walls.



(a) Proposed method (b) Hybrid FE-SEA method (c) Monte Carlo Simulation

Fig. 3 The models of the acoustic cavity employed in the three methods

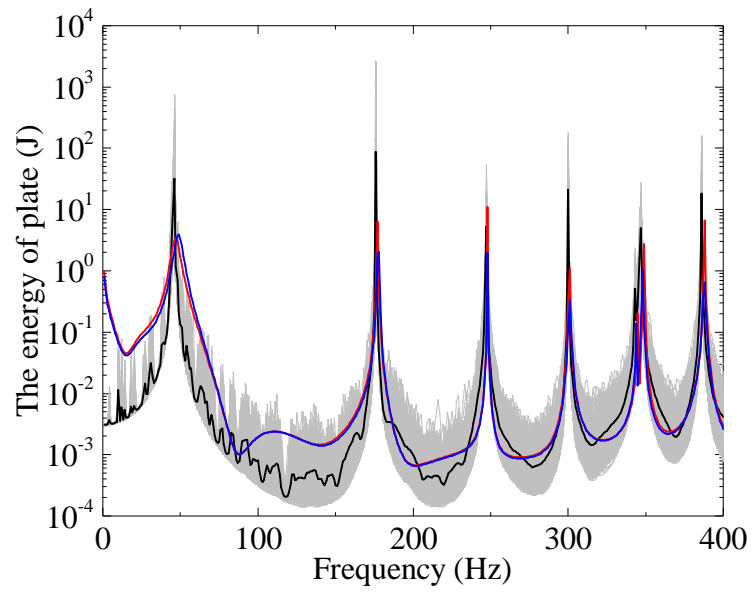
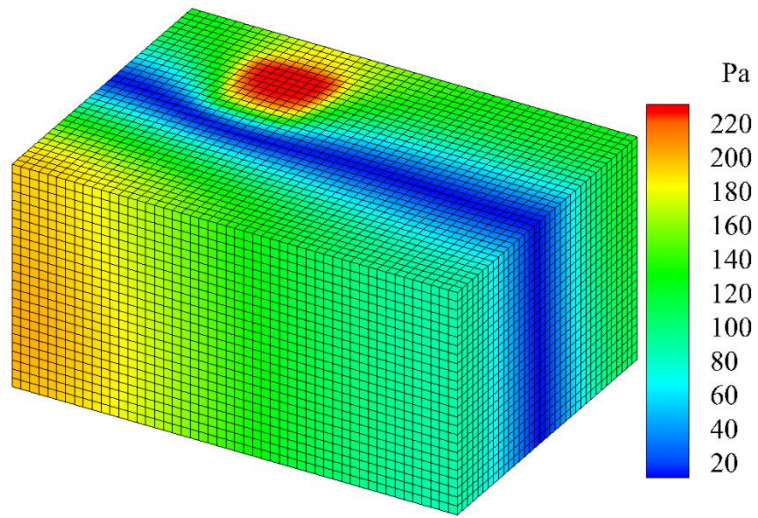
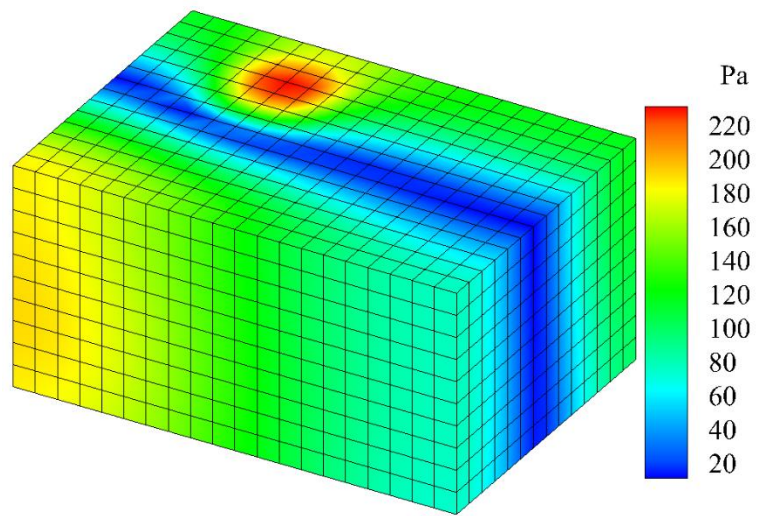


Fig. 4 Energy in the plate. Gray lines, computed using Monte Carlo approach for 500 realizations of ensemble; black line, ensemble average of Monte Carlo results; red line, ensemble average computed using Hybrid FE-SEA method; blue line, ensemble average computed using Hybrid BE-SEA method.



(a) Monte Carlo simulation



(b) Proposed method

Fig. 5 Sound pressure contour on the boundary of acoustic cavity.

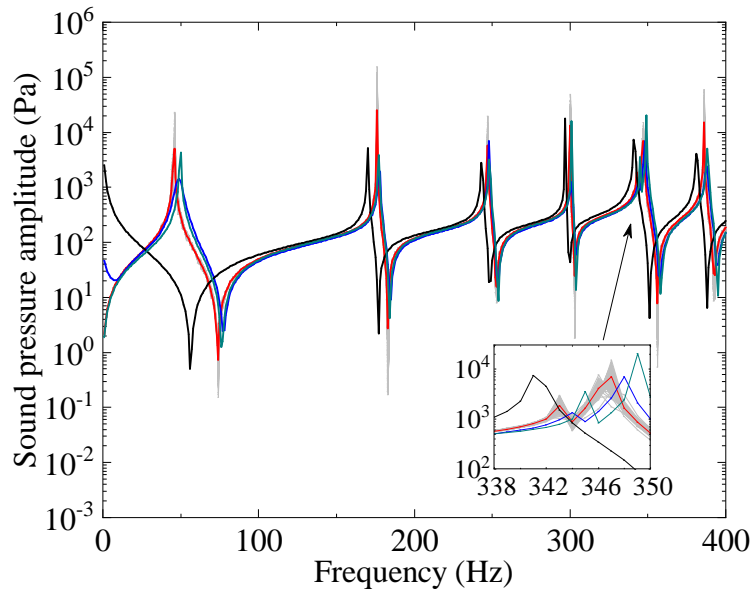


Fig. 6 Sound pressure response at the center of the domain subjected to external excitation. Gray lines, computed using Monte Carlo approach for 500 realizations of ensemble; red line, ensemble average of Monte Carlo results; blue line, ensemble average computed using Hybrid BE-SEA method; black line, computed using a fully deterministic FE model considering the plate as a rigid plate; dark cyan line, computed using a fully deterministic FE model considering the plate as a homogenous plate with the nominal thickness provided by this paper.

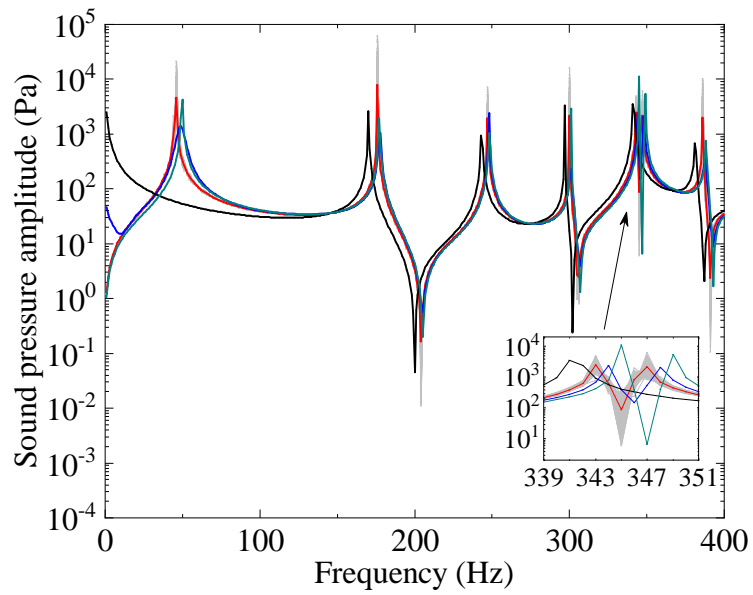


Fig. 7 Sound pressure response at a point inside the acoustic cavity with coordinates (0.40, 0.60, 0.30). Gray lines, computed using Monte Carlo approach for 500 realizations of ensemble; red line, ensemble average of Monte Carlo results; blue line, ensemble average computed using Hybrid BE-SEA method; black line, computed using a fully deterministic FE model considering the plate as a rigid plate; dark cyan line, computed using a fully deterministic FE model considering the plate as a homogenous plate with the nominal thickness provided by this paper.